

Design and Synthesis of Skeletal Analogues of Gambierol: Attenuation of Amyloid- β and Tau Pathology with Voltage-Gated Potassium Channel and *N*-Methyl-D-aspartate Receptor Implications

Eva Alonso,[†] Haruhiko Fuwa,[‡] Carmen Vale,[†] Yuto Suga,[‡] Tomomi Goto,[‡] Yu Konno,[‡] Makoto Sasaki,[‡] Frank M. LaFerla,^{||} Mercedes R. Vieytes,[§] Lydia Giménez-Llort,[⊥] and Luis M. Botana^{*,†}

[†]Departamento de Farmacología, Facultad de Veterinaria, Universidad de Santiago de Compostela, Lugo, Spain

[‡]Graduate School of Life Sciences, Tohoku University, 2-1-1 Katahira, Aoba-ku, Sendai 980-8577, Japan

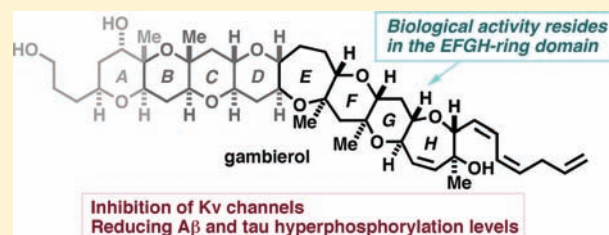
[§]Departamento de Fisiología, Facultad de Veterinaria, Universidad de Santiago de Compostela, 27003 Lugo, Spain

^{||}Department of Neurobiology and Behavior, University of California, Irvine, Irvine, California 92697, United States

[⊥]Departamento de Psiquiatría y Medicina Legal, Instituto de Neurociencias, Universidad Autonoma de Barcelona, 08193 Bellaterra, Spain

S Supporting Information

ABSTRACT: Gambierol is a potent neurotoxin that belongs to the family of marine polycyclic ether natural products and primarily targets voltage-gated potassium channels (K_v channels) in excitable membranes. Previous work in the chemistry of marine polycyclic ethers has suggested the critical importance of the full length of polycyclic ether skeleton for potent biological activity. Although we have previously investigated structure–activity relationships (SARs) of the peripheral functionalities of gambierol, it remained unclear whether the whole polycyclic ether skeleton is needed for its cellular activity. In this work, we designed and synthesized two truncated skeletal analogues of gambierol comprising the EFGH- and BCDEFGH-rings of the parent compound, both of which surprisingly showed similar potency to gambierol on voltage-gated potassium channels (K_v) inhibition. Moreover, we examined the effect of these compounds in an in vitro model of Alzheimer's disease (AD) obtained from triple transgenic (3xTg-AD) mice, which expresses amyloid beta ($A\beta$) accumulation and tau hyperphosphorylation. In vitro preincubation of the cells with the compounds resulted in significant inhibition of K^+ currents, a reduction in the extra- and intracellular levels of $A\beta$, and a decrease in the levels of hyperphosphorylated tau. In addition, pretreatment with these compounds reduced the steady-state level of the *N*-methyl-D-aspartate (NMDA) receptor subunit 2A without affecting the 2B subunit. The involvement of glutamate receptors was further suggested by the blockage of the effect of gambierol on tau hyperphosphorylation by glutamate receptor antagonists. The present study constitutes the first discovery of skeletally simplified, designed polycyclic ethers with potent cellular activity and demonstrates the utility of gambierol and its synthetic analogues as chemical probes for understanding the function of K_v channels as well as the molecular mechanism of $A\beta$ metabolism modulated by NMDA receptors.



INTRODUCTION

Ever since the isolation and structure determination of brevetoxin-B by Nakanishi and his colleagues,¹ marine polycyclic ether natural products have continuously been fascinating to the scientific community due to their extraordinary complex molecular architecture and diverse and potent biological activities.² The representative members of the family of marine polycyclic ether natural products are brevetoxins (PbTx), ciguatoxins, maitotoxin, and gambierol, which are known to exhibit high neurotoxicity against mammals.³ Gambierol (1, Figure 1), one of the toxic secondary metabolites produced by the dinoflagellate *Gambierdiscus toxicus*, was isolated and structurally characterized by Satake, Yasumoto, and co-workers.⁴ The Satake/Yasumoto group has reported that gambierol exhibits potent acute lethal toxicity against mice (minimal lethal dose: 50 $\mu\text{g}/\text{kg}$, ip) and

their neurological symptoms resemble those shown by ciguatoxins, the principal responsible toxin for ciguatera seafood poisoning, although the natural scarcity of gambierol has hampered for many years further detailed investigations into its biological activity. However, recent total syntheses by several groups have made sufficient quantities of synthetic material available.^{5–8} Moreover, preliminary structure–activity relationship (SAR) investigations involving in vivo evaluation of synthetic analogues have shown that both the triene side chain and the H-ring functional groups are essential for the potent toxicity.⁹ However, there remains an important question whether the ladder-shaped polycyclic ether skeleton as a whole is necessary for the biological activity.

Received: January 18, 2012

Published: April 4, 2012

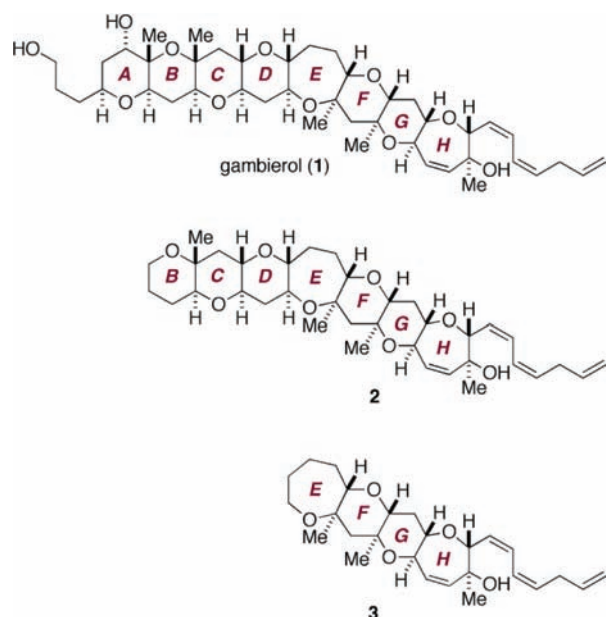


Figure 1. Structures of gambierol **1**, heptacyclic analogue **2**, and tetracyclic analogue **3**.

Voltage-gated potassium channels (K_v) have been shown to be the primary molecular targets of the toxin.¹⁰ Among the potassium channel subtypes tested, the evaluation of **1** in mammalian Kv1.1-Kv1.6, hERG, and insect Shaker IR subtypes showed Kv1.2 channels as the most sensitive one with an IC_{50} of about 15 nM and a 98% of inhibition¹⁰ and did not affect TRPV1 channels. However, the compound also exhibited moderate inhibitory activity against voltage-gated sodium channels (Na_v) and modified calcium homeostasis,^{11,12} but it did not have effect over the mammalian Nav1.1-Nav1.8 channels and insect Para at concentrations up to 1 μ M, nor on sodium currents in taste cells at concentrations in the nanomolar range.¹⁰ Our previous work has shown that gambierol induced synchronous calcium oscillations in the presence of extracellular calcium ion in primary cerebellar neurons, which were completely abolished by the selective NMDA receptor antagonist D-(−)-2-amino-5-phosphonopentanoate (APV) and by the glutamate release inhibitor riluzole.¹³ Similar effects were observed with 4-aminopyridine (4-AP) that has been shown to modulate the function of NMDA receptors via inhibition of K_v channels. Thus, our results indicated that gambierol-evoked Ca^{2+} oscillations in cerebellar neurons would involve modulation of NMDA receptors, which are most likely secondary to K_v channel inhibition.

Meanwhile, recent studies on the mechanism of the amyloid- β ($A\beta$) metabolism, possibly responsible for the molecular pathology of Alzheimer's disease (AD), demonstrated that NMDA receptors play a significant role in the regulation of amyloid- β precursor protein (APP) expression and $A\beta$ production.¹⁴ Histopathologically, AD is characterized by two main hallmarks, deposition of insoluble $A\beta$ peptide in senile plaques and intracellular neurofibrillary tangles derived from hyperphosphorylated tau proteins.¹⁵ $A\beta$ is produced by the abnormal proteolytic cleavage of APP, principally by two enzymes, β -secretase (BACE) and γ -secretase (presenilin 1 and 2). These enzymes sequentially cleave APP in the N- and C-terminal end, respectively, generating 39–43 amino acid polypeptides with limited solubility, which aggregate and form

$A\beta$ deposits.¹⁶ The $A\beta$ plaques appear in determinate brain regions and produce neuronal death, inflammatory response and a progressive cognitive failure.¹⁷ On the other hand, neurofibrillary tangles are formed predominantly from hyperphosphorylated isoforms of the tau protein, a microtubule-associated protein.¹⁸ In normal cells, tau function is to promote the polymerization of tubulin for the formation of microtubules.¹⁹ Phosphorylation of tau can alter the correct axonal transport and neuronal structure, leading to neuronal degeneration.²⁰

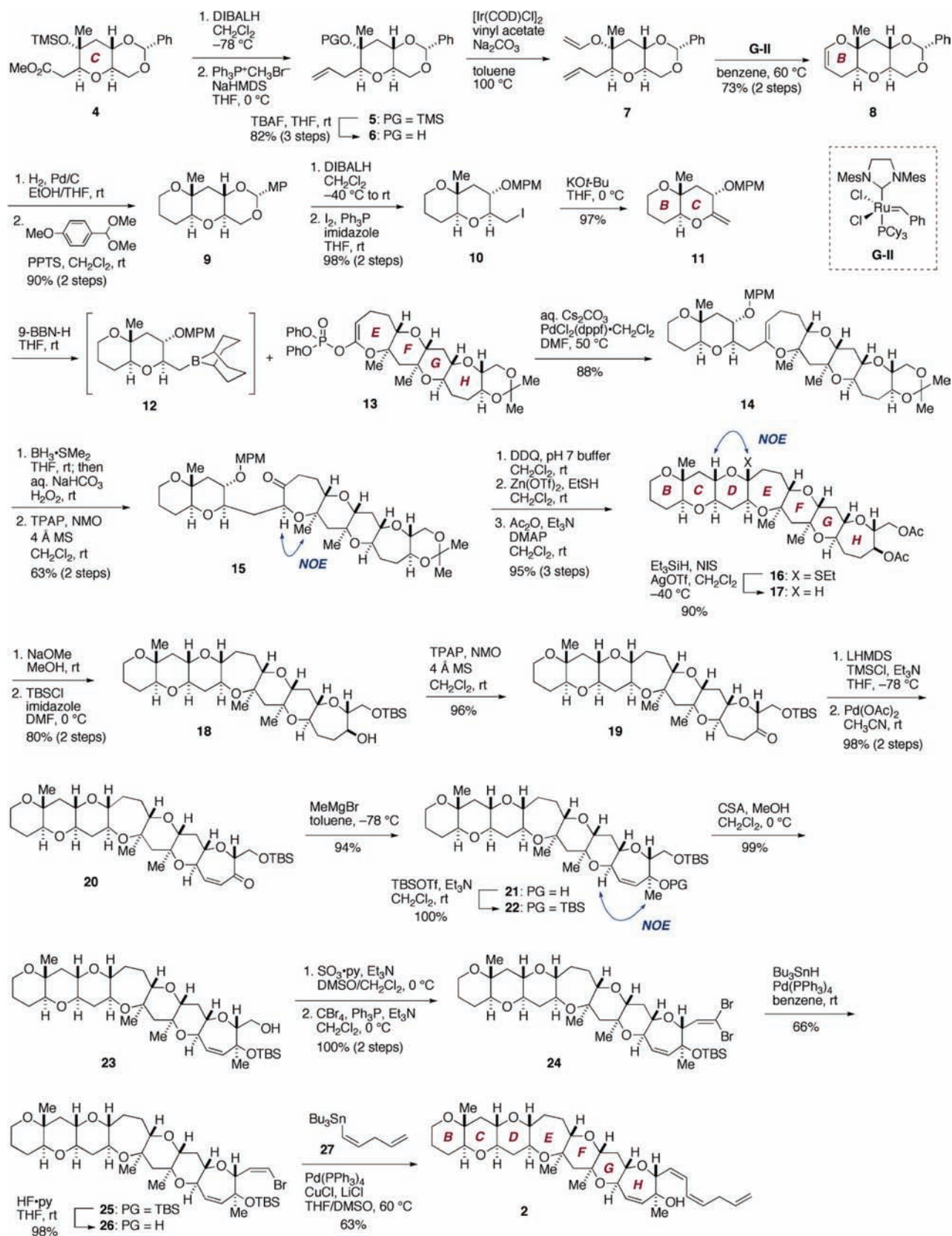
The cellular effects of gambierol on K_v channels and NMDA receptors²¹ as well as the involvement of NMDA receptors in APP expression and $A\beta$ production led us to pursue the following three objectives in this work: (i) design and synthesis of truncated skeletal gambierol analogues, (ii) comparison of the effects of gambierol and its skeletal analogues on K_v channels, and (iii) analysis of the effects of gambierol and analogues in an in vitro model of AD obtained from 3xTg-AD mice with simultaneous overexpression of $A\beta$ and hyperphosphorylation of tau.²²

RESULTS

Chemical Synthesis of Gambierol Analogues. The synthesis of the heptacyclic analogue **2** (Figure 1) commenced with reduction of the known ester **4**²³ that corresponds to the C-ring of **1** (Scheme 1). Wittig methylation of the derived aldehyde and removal of the silyl group gave alcohol **6**. For the construction of the B-ring tetrahydropyran, ring-closing metathesis²⁴ of vinyl ether **7** was envisioned. However, vinylation of sterically encumbered tertiary alcohol **6** turned out to be nontrivial, as the Hg(II)-mediated²⁵ or Pd(II)-catalyzed²⁶ transesterifications only gave disappointing results. We found that iridium-catalyzed vinylation protocol developed by Ishii and co-workers²⁷ worked well with **6** to deliver **7**, which upon exposure to the Grubbs second-generation catalyst (**G-II**)²⁸ (benzene, 60 °C) led to dihydropyran **8**. A slight modification of the Ishii conditions was required to achieve satisfactory conversion in the vinylation process. Hydrogenation/hydrogenolysis of **8** followed by acetalization provided *p*-methoxybenzylidene acetal **9**. Regioselective reductive opening of the acetal, iodination, and subsequent base treatment afforded exocyclic enol ether **11**.

Toward the construction of the heptacyclic polyether skeleton, we exploited the Suzuki–Miyaura coupling-based methodology developed in our laboratory.^{29,30} Hydroboration of **11** with 9-BBN-H delivered alkylborane **12**, which without isolation was reacted with the EFGH-ring enol phosphate **13**⁵ in the presence of aqueous Cs_2CO_3 and $PdCl_2(dppf) \cdot CH_2Cl_2$ catalyst to furnish enol ether **14** in 88% yield. Hydroboration of **14** with $BH_3 \cdot SMe_2$ followed by oxidative workup gave an inseparable 3:1 mixture of diastereomeric alcohols, which was oxidized³¹ to provide ketone **15**, after removal of the minor diastereomer (not shown) by flash chromatography on silica gel. The stereochemistry of **15** was unambiguously established by an NOE experiment as shown. Deprotection of the *p*-methoxybenzylmethyl (MPM) group, mixed thioacetalization,³² and acylation of the liberated hydroxy groups afforded mixed thioacetal **16**. Unexpectedly, stereoselective reduction of mixed thioacetal **16** proved to be a challenging task. Reduction of **16** under tin hydride conditions ($n-Bu_3SnH$, AIBN, toluene, 100 °C) gave heptacycle **17** in 57% yield, along with the undesired epimer (not shown) in 24% yield (12% recovery of **16**). On the other hand, oxidation of mixed thioacetal **16** with *m*-CPBA followed by in situ treatment with $Et_3SiH/BF_3 \cdot OEt_2$ ³³ resulted in a complete

Scheme 1. Synthesis of the Heptacyclic Analogue 2



diastereoselective reduction to give **17** in approximately 73% yield, albeit an unidentified byproduct contaminated that could not be separated until the end of the synthesis. Eventually, we resorted to a new method for the reduction of mixed thioacetal **16**. Thus,

activation of **16** with *N*-iodosuccinimide (NIS)/AgOTf³⁴ in the presence of Et₃SiH (CH₂Cl₂, -40 °C) cleanly afforded **17** in 90% yield as a single stereoisomer. The stereochemistry of **17** was determined by an NOE experiment as shown.

Scheme 2. Synthesis of the Tetracyclic Analogue 3

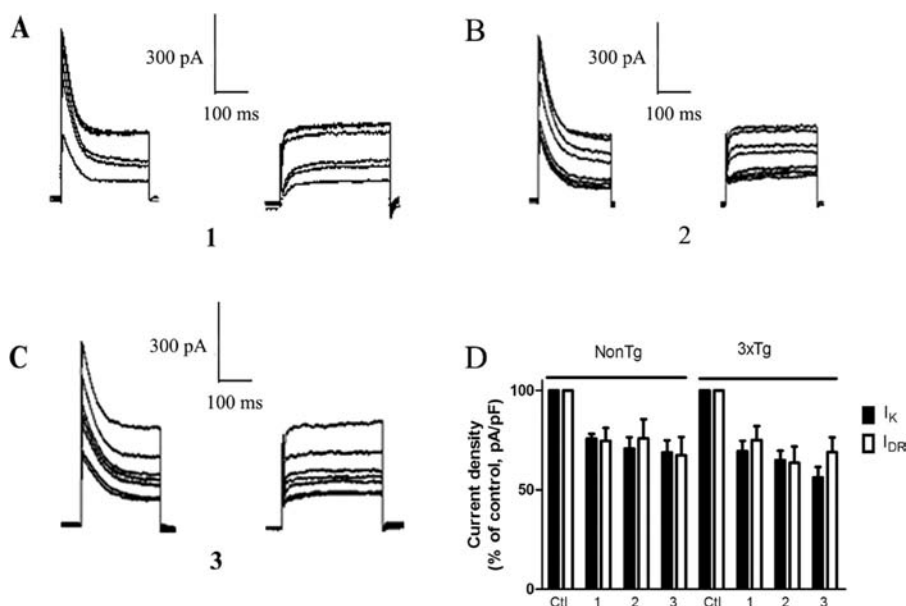
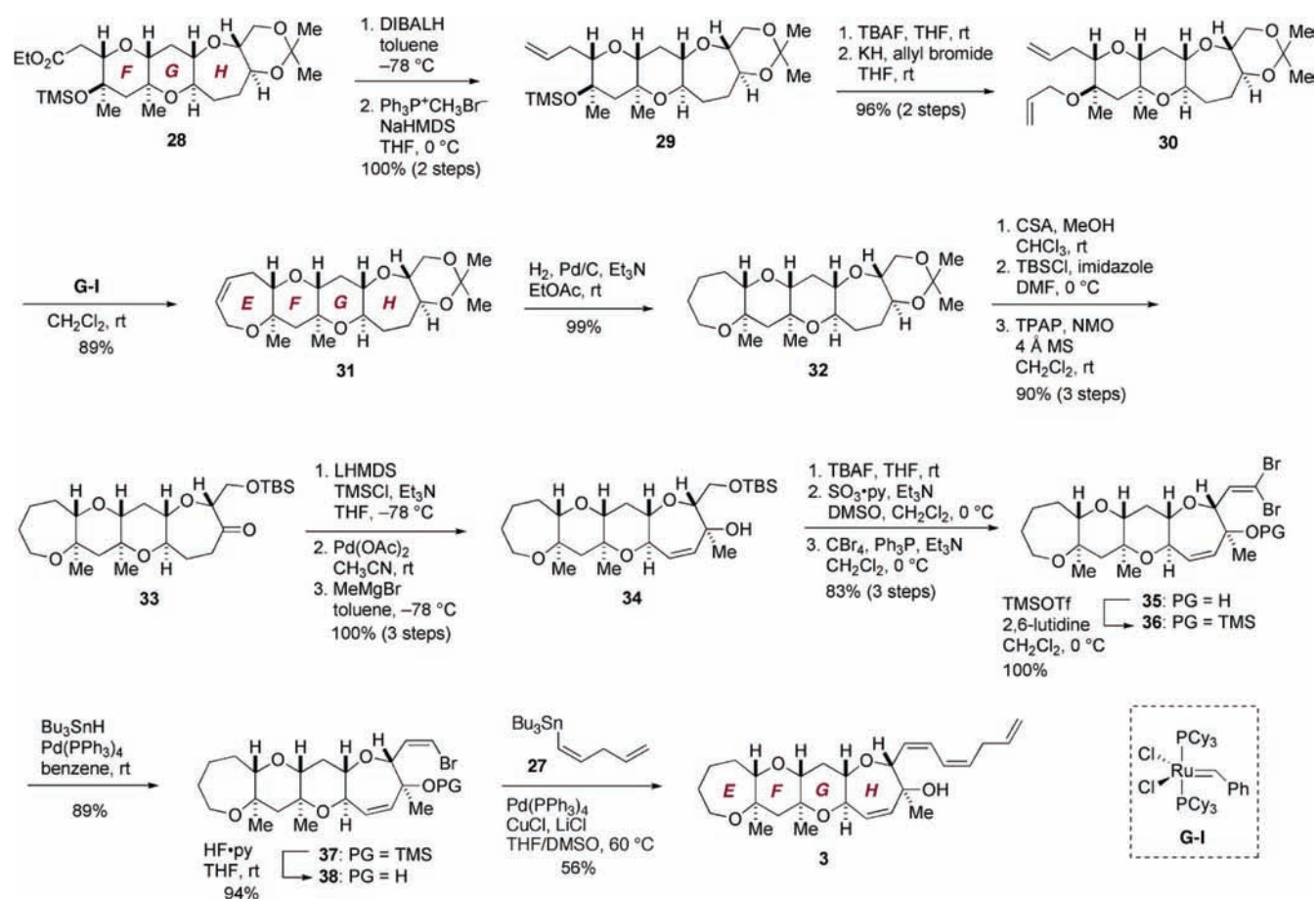


Figure 2. Effect of bath application of 1, 2, or 3 on potassium currents in nontreated neurons. (A–C) Representative electrophysiological recordings showing the concentration–response effect 5 min after administration of 1 (A), 2 (B), and 3 (C) to the extracellular solution over the I_K and I_{DR} components of K^+ currents in 3xTg-AD neurons at concentrations of 0.1, 1, 10, 100, 500, and 1000 nM. The holding potential was -80 mV. Recordings are from the same cell with the different concentrations of each compound. (D) Quantitative analysis of the inhibition of I_K and I_{DR} current densities (pA/pF) in the presence of 1, 2, or 3 at 100 nM in NonTg and 3xTg-AD neurons. Results are mean \pm SEM of 6–14 cells.

Removal of the acetyl groups and selective silylation of the liberated primary alcohol gave alcohol 18, which was oxidized to provide ketone 19. The double bond of the H-ring was

introduced according to the Saegusa–Ito protocol³⁵ to yield enone 20, which was reacted with MeMgBr ³⁶ to deliver alcohol 21 as a single stereoisomer. The stereochemistry of 21 was

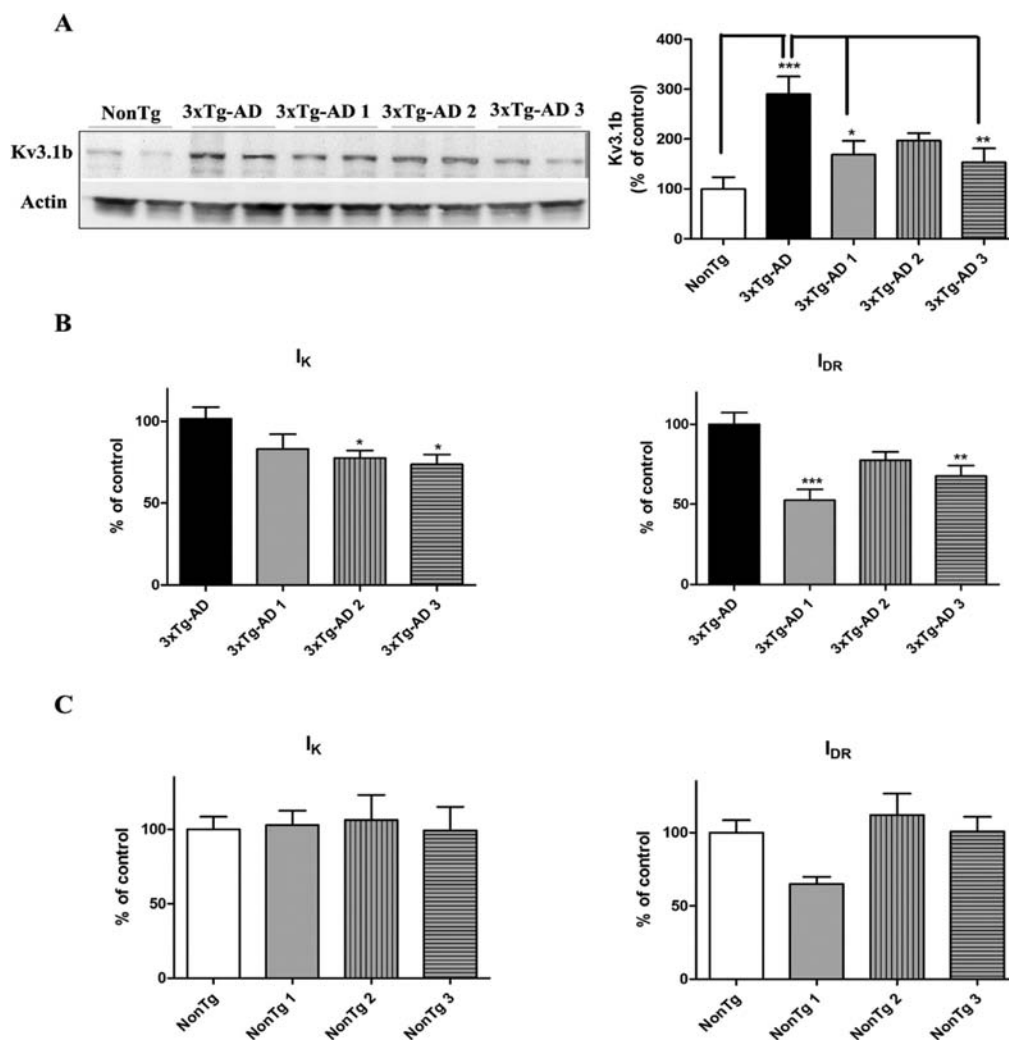


Figure 3. Chronic treatments with **1**, **2**, or **3** reduced the overexpression of the $K_v3.1$ subunit and the amplitude of potassium currents. (A) Representative Western blot and the corresponding histogram showing $K_v3.1$ expression levels in NonTg, 3xTg-AD, and 3xTg-AD neurons treated with gambierol and the two analogues as measured with the $K_v3.1$ antibody which recognizes a full-length $K_v3.1$ protein and does not cross react with any other potassium channel antigens. Results are mean \pm SEM of 5 experiments, each performed in duplicate. (B) Effect of long-term exposure from 3 to 7 div to **1**, **2**, or **3** in the amplitude of I_K and I_{DR} currents in 3xTg-AD cortical neurons. (C) Effect of long-term exposure from 3 to 7 div to **1**, **2**, or **3** in the amplitude of I_K and I_{DR} currents in NonTg neurons. Results are mean \pm SEM of 6–14 cells. * $p < 0.05$ and *** $p < 0.001$.

established by an NOE experiment. Silylation followed by selective cleavage of the primary silyl ether under acidic conditions gave alcohol **23**, which was oxidized and then converted to dibromoolefin **24**. Selective reduction of **24** ($n\text{-Bu}_3\text{SnH}$, $\text{Pd}(\text{PPh}_3)_4$)³⁷ led to (*Z*)-vinyl bromide **25**, which was desilylated with HF-pyridine to provide alcohol **26**. Finally, Stille coupling³⁸ of **26** with vinyl stannane **27** ($\text{Pd}(\text{PPh}_3)_4$, CuCl , LiCl , DMSO/THF , $60\text{ }^\circ\text{C}$)⁹ furnished heptacyclic analogue **2**.

The synthesis of the tetracyclic analogue **3** (Figure 1) started with the known ester **28**⁵ that represents the FGH-ring framework of **1** (Scheme 2). DIBALH reduction of **28** and ensuing Wittig methylenation gave olefin **29**, which was transformed to diene **30** via desilylation and allylation. Ring-closing metathesis of **30** proceeded cleanly in the presence of the Grubbs first-generation catalyst (**G-I**)⁴⁰ to deliver oxepene **31**. Hydrogenation of **31** gave pentacycle **32** in nearly quantitative yield. Removal of the acetonide under acidic conditions, selective silylation of the unmasked primary hydroxy group, and subsequent oxidation led to ketone **33**. This was elaborated to tetracyclic analogue **3** in a similar manner as that described for **2**.

Effect of Gambierol and Its Synthetic Analogues on Voltage-Gated Potassium Channels.

With **2** and **3** in hand (Figure 1), we evaluated their cellular activity and compared it to that of **1**. Since the effect of acute administration of **1** and synthetic analogues on K^+ currents was not previously evaluated in cortical neurons, we first analyzed the effect of the acute application of these compounds in this neuronal model. As shown in Figure 2A–C, application of gambierol or analogues to primary cortical neurons produced a concentration-dependent inhibition of K^+ current densities. Thus, **1**, **2**, and **3** at 100 nM inhibited I_K currents in 3xTg-AD neurons to a $69.4 \pm 5.1\%$, $64.8 \pm 4.0\%$, and $56.1 \pm 5.0\%$, respectively, versus control currents, and the I_{DR} component to a $75.0 \pm 7.1\%$, $63.6 \pm 8.1\%$, and $68.5 \pm 7.0\%$. Similar results were found in NonTg cortical neurons where, at the same concentration, I_K current density was inhibited to a $75.7 \pm 2.0\%$, $70.7 \pm 5.0\%$, and $68.7 \pm 6.1\%$ by **1**, **2**, and **3**, respectively, while the I_{DR} component was blocked to a $74.6 \pm 6.0\%$, $75.7 \pm 9.6\%$, and $67.3 \pm 9.0\%$, respectively, versus control currents as summarized in Figure 2D.

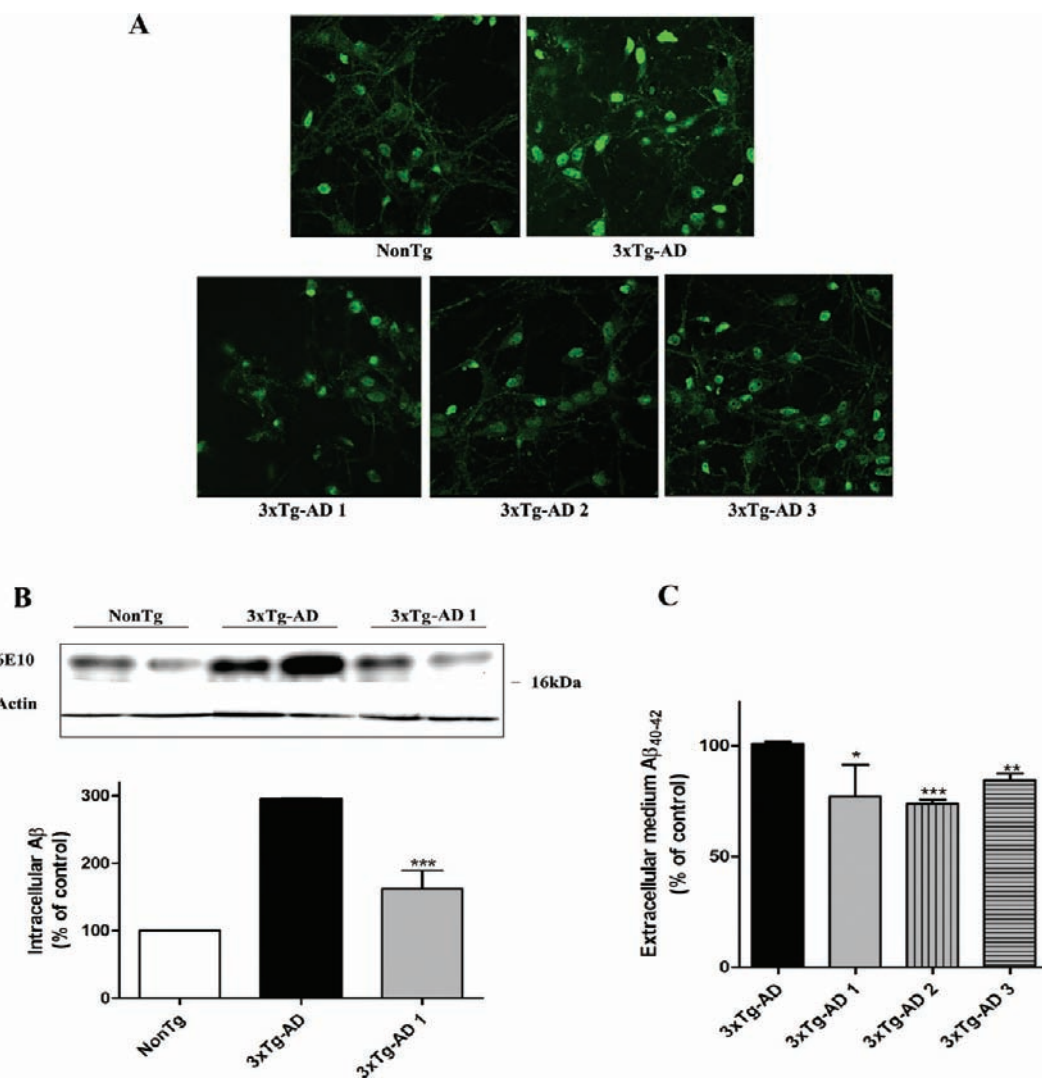


Figure 4. Gambierol (**1**) and its analogues **2** and **3** decreased intra- and extracellular accumulation of A β . (A) Confocal microscopy images of the immunoreactivity for the 6E10 antibody, which reacts with abnormally processed isoforms and precursor forms of the protein, employed to measure intracellular A β levels and corresponding quantitative analysis in NonTg, 3xTg-AD, and 3xTg-AD neurons treated with **1**, **2**, or **3** from third to seventh div. Scale bar is 20 μ m. (B) Representative Western blot bands indicating intracellular A β levels in NonTg neurons, 3xTg-AD neurons, and 3xTg-AD neurons treated with **1** and probed with the 6E10 antibody. Quantification of Western blot band intensities for A β levels as obtained from 3 independent experiments, performed in duplicate. *** p < 0.0001 versus 3xTg-AD neurons. (C) Quantitative analysis of the levels of extracellular A β measured in the culture medium after treatment of the neurons with **1**, **2**, or **3** from the third to the seventh div. Results are mean \pm SEM of 3–5 independent experiments each performed in duplicate. * p < 0.05, ** p < 0.01 and *** p < 0.001.

Cytotoxic Evaluation of Gambierol and Its Synthetic Analogues in Cortical Neurons. Previous work in our laboratory has shown that **1** modified the intracellular calcium concentration in a way dependent on glutamate signaling and that the toxin also inhibited K⁺ currents in cerebellar granule neurons.¹³ Glutamate signaling is related to neurodegenerative diseases, and glutamate receptors and their excitotoxic effects are being widely studied in AD.⁴¹ Therefore, the effect of **1**, **2**, and **3** was evaluated in an in vitro model of primary cortical neurons obtained from 3xTg-AD mice, a model known to overexpress A β and hyperphosphorylated tau.²² First, the in vitro toxicity of the compounds was evaluated by the MTT assay after exposing neuronal cultures to the compounds from 3 to 7 days in vitro. **1** and **3** did not show any cytotoxicity even at 10 μ M (105.8 \pm 6.27% of control) and at 5 μ M (101.5 \pm 4.6% of control), respectively. In contrast, **2** showed a decrease in cellular viability, a 46.2 \pm 0.5% of cellular viability for 1 μ M and a

79.5 \pm 10.0% for 0.5 μ M. However, it showed no cytotoxic effects at concentrations below 500 nM, showing a viability of 124.4 \pm 8.1% with respect to control cells. In the following experiments, we used nontoxic concentrations of the compounds. Thus, 3xTg-AD neurons were pretreated with **1** at 10 μ M, **2** at 100 nM, and **3** at 5 μ M. Treatments were made in the culture medium from the third div (days in vitro) to the seventh div. Control cells were treated with the corresponding concentration of the vehicle, DMSO.

Long-Term Exposure of Cortical Neurons to Gambierol and Its Truncated Skeletal Analogues Decreases Voltage-Gated Potassium Currents. Since it has been observed that acute application of **1** at nanomolar concentrations inhibited K⁺ currents and that the toxin strongly suppressed K_v3.1 dependent currents with higher potency than K_v2 or K_v4 currents,²¹ we analyzed the long-term effects of the exposure of cortical neurons to **1** on K_v3.1 expression and K⁺

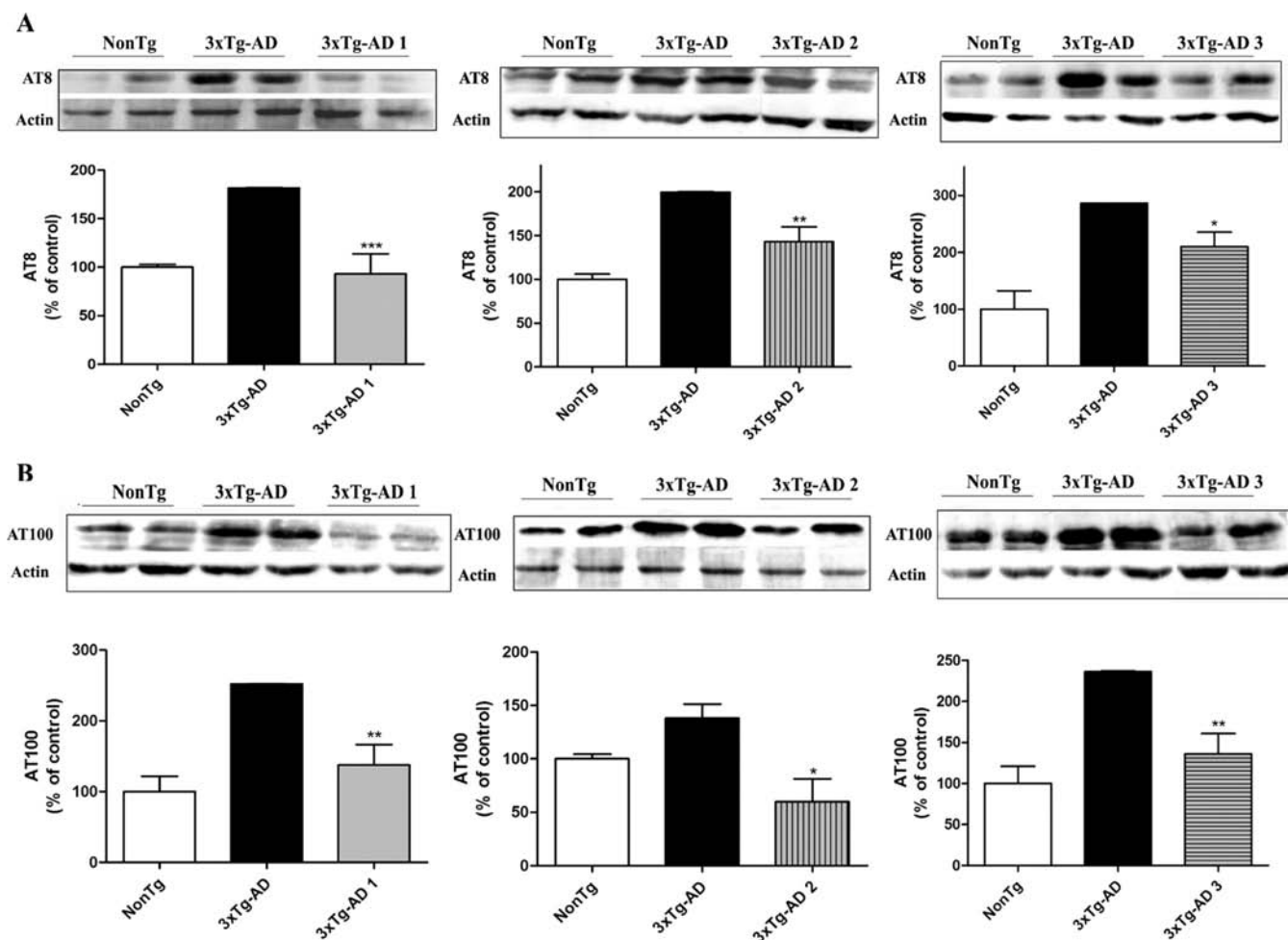


Figure 5. Chronic exposure of 3xTg-AD neurons to 1, 2, or 3 decreased tau phosphorylation. (A) Representative Western blot bands probed with the AT8 antibody (which recognizes a tau epitope doubly phosphorylated at serine 202 and threonine 205 and does not cross-react with normal tau sequences) in control, 3xTg-AD, and 3xTg-AD treated neurons. Quantitative analysis of AT8 levels in control, 3xTg-AD neurons, and 3xTg-AD treated neurons. (B) Representative Western blot bands indicating phospho-tau levels in control, 3xTg-AD, and 3xTg-AD treated neurons probed with the AT100 antibody (which recognizes tau phosphorylated at serine 212 and threonine 214). Quantification of AT100 levels in control, 3xTg-AD neurons, and 3xTg-AD treated neurons. Results are mean \pm SEM of 3 experiments, each performed in duplicate. $^{*}p < 0.01$ versus 3xTg-AD neurons. $^{***}p < 0.001$ versus 3xTg-AD neurons.

current amplitude in this 3xTg-AD primary cortical model. As shown in Figure 3A, 3xTg-AD neurons in culture presented an overexpression of the $K_v3.1$ channel. Immunoblotting analysis with a specific antibody for this K_v subtype on cellular lysates and its corresponding densitometry showed a significant increase in the band intensity corresponding to 3xTg-AD cortical neurons lysates versus control NonTg neurons (control, $100 \pm 23.6\%$; 3xTg-AD, $290.3 \pm 35.2\%$ ($p = 0.0012$)), as shown in Figure 3A. Treatment of the 3xTg-AD neurons with 1, 2, or 3 from the third to the seventh div decreased the $K_v3.1$ up-regulation (Figure 3A). Next, electrophysiological recordings were performed to evaluate the functional relevance of potassium channels in the in vitro AD model. The I_K current in 3xTg-AD neurons was partially abolished by the skeletal analogues but not significantly by 1. As shown in Figure 3B, in 3xTg-AD neurons treated with 3, the total outward current I_K was $26.3 \pm 6.0\%$ smaller than that in nontreated neurons and $22.4 \pm 4.5\%$ for 2, while the inhibition of I_K by 1 was $16.8 \pm 9.1\%$. On the other hand, exposure of cortical neurons to 1, 2, or 3 showed a similar effect on the I_{DR} component. Thus, in neurons treated with 1, I_{DR} was $47.5 \pm 6.8\%$ smaller than that in nontreated 3xTg-AD neurons, whereas in 3xTg-AD neurons

cultured in the presence of 2 or 3, I_{DR} was decreased by $32.4 \pm 6.5\%$ or $22.5 \pm 5.1\%$, respectively. In agreement with the overexpression of $K_v3.1$ channels in 3xTg-AD neurons observed by the Western blot experiments, the size of K^+ currents was smaller in NonTg cells with respect to 3xTg-AD. Thus, the amplitude of the I_K current was 607.8 ± 44.1 pA in nontreated 3xTg-AD neurons and 471.3 ± 79.6 pA in nontreated NonTg neurons, while for the I_{DR} component, the amplitude of the current was 450.6 ± 39.6 pA in 3xTg-AD neurons and 316.2 ± 37.7 pA in NonTg cells. Unexpectedly, only long-term exposure to 1 inhibited the I_{DR} current in normal neurons, whereas the total outward current was unaffected (Figure 3C).

Gambierol Effects in $A\beta$ and Tau Cellular Pathologies.

In view of the effects of 1–3 on the expression of $K_v3.1$ channels and on the K^+ currents, we analyzed if these compounds could affect the intra- and extracellular $A\beta$ accumulation levels observed in 3xTg-AD neurons in culture. Western blot and confocal microscopy employing the 6E10 antibody were used for quantifying intracellular $A\beta$ levels. As shown in Figure 4A, all the compounds significantly reduced the immunoreactivity of 3xTg-AD neurons to 6E10 antibody. To confirm these data, Western blot experiments were performed

after treatment of cortical neurons with **1**. As shown in Figure 4B, cortical 3xTg-AD cultures grown in the presence of **1** from the third to seventh div, showed a significant decrease in intracellular $A\beta$ accumulation after treatment with **1** ($45.2 \pm 9.3\%$; $p = 0.003$). Since extracellular $A\beta_{40-42}$ is also increased in 3xTg-AD neurons in culture,²² we checked if the intracellular decrease of $A\beta$ was accompanied with a decrease in $A\beta$ accumulation in the extracellular medium. Collected samples of culture medium with and without compounds were analyzed by BetaMark x-42 ELISA kit (SIGNET), a colorimetric ELISA kit. As it can be seen in Figure 4C, the compounds slightly reduced the amount of $A\beta_{40-42}$ in the extracellular culture medium, that is, **1** in $23.0 \pm 10.1\%$ ($p = 0.003$), **2** in $26.18 \pm 1.8\%$ ($p < 0.001$), and **3** in $15.7 \pm 3.1\%$ ($p < 0.01$).

Inhibition of $A\beta$ accumulation delays the progression of tau pathology in vivo.⁴² Moreover, $A\beta$ oligomers can stimulate tau phosphorylation in vitro⁴³ and $A\beta$ and tau can also form complexes that enhance tau phosphorylation by GSK-3 β .⁴⁴ Therefore, we evaluated whether gambierol and its analogues could modify tau expression. As shown in Figure 5, all the compounds decreased the immunoreactivity levels of AT8 and AT100 antibodies by 30–50% after exposure of 3xTg-AD cultures to the compounds. AT8 recognizes tau proteins phosphorylated at Ser 202, while AT100 binds to tau proteins phosphorylated at Thr 212 and Ser 214. These are the two of representative antibodies used in the study of tau hyperphosphorylation in AD. As shown in Figure 5A, treatment of 3xTg-AD cortical cultures with **1**, **2**, or **3** decreased phosphorylated tau levels for the two antibodies. For AT8, the immunoreactivity decreased in $51.2 \pm 11.4\%$ ($p < 0.001$), $28.3 \pm 8.2\%$ ($p < 0.01$), and $26.6 \pm 6.3\%$ ($p < 0.05$) by exposure to **1**, **2**, and **3**, respectively. For AT100, the decreases were $45.4 \pm 11.4\%$ ($p = 0.0037$), $56.5 \pm 19\%$ ($p < 0.05$), and $42.4 \pm 10.4\%$ ($p = 0.0034$) for **1**, **2**, and **3**, respectively (Figure 5B).

Involvement of Glutamate Signaling on Gambierol Effects against $A\beta$ and Tau Pathologies. We have previously shown that, in cerebellar granule neurons, acute administration of **1** elicited calcium oscillations that were abolished by the application of APV, a specific NMDA receptor antagonist, and by riluzole, a glutamate release inhibitor, suggesting that glutamate signaling was involved in the effect of **1**.¹³ To evaluate the involvement of glutamate signaling in the beneficial effect of **1** against $A\beta$ and tau pathology, we examined the effects of the pretreatment of 3xTg-AD cortical neurons with **1** in the intracellular calcium response elicited by application of $50 \mu\text{M}$ glutamate. In 3xTg-AD neurons, long-term exposure to **1** showed no difference in the glutamate induced calcium response respect to 3xTg-AD nontreated neurons (Figure 6A). In addition, the effect of **1–3** on glutamate excitotoxicity was evaluated by adding $100 \mu\text{M}$ glutamate to the culture medium after a 24 h-pretreatment with **1**, **2**, or **3**. Thus, the cells were incubated for additional 48 h and then cellular viability was evaluated by the MTT test. As expected, glutamate application reduced cellular viability by $25.4 \pm 6.8\%$,^{45,46} but neither **1**, **2**, nor **3** modified the decrease in cell viability produced by glutamate in control NonTg and 3xTg-AD neurons (Figure 6B).

Previous studies in our laboratory have shown that calcium effects induced by **1** were abolished by NMDA modulators.¹³ Therefore, we also investigated if the cellular expression of the NMDA receptor and the closely linked mGlu5 receptor (metabotropic glutamate receptor 5) were affected by long-term exposure of cortical 3xTg-AD neurons to **1**, **2**, or **3**. As shown in Figure 7A, pretreatment of 3xTg-AD cells with the compounds

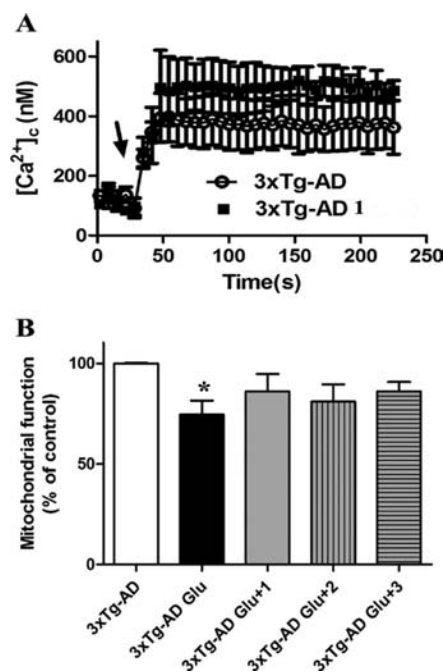


Figure 6. Effect of **1**, **2**, and **3** on glutamate-induced neurotoxicity and the calcium response elicited by glutamate. (A) Chronic exposure of cortical neurons to $10 \mu\text{M}$ of **1** did not modify the calcium response elicited by addition of $50 \mu\text{M}$ glutamate (indicated by the arrow) when compared with the response evoked by glutamate in nontreated neurons. (B) Glutamate-induced toxicity in primary cortical neurons from control and 3xTg-AD mice was not affected by pretreatment of the neurons with either **1**, **2**, or **3** as evaluated by the MTT reduction assay. * $p < 0.05$ versus NonTg cells. Data are mean \pm SEM of 3 independent experiments, each performed in duplicate.

induced a decrease in band intensity obtained by Western blot with the NMDA receptor subunit N2A antibody. Although no differences in N2A expression between control and 3xTg-AD neurons were found, a diminishment in N2A expression of $37.7 \pm 2.9\%$ was found after exposure of cortical neurons to **1**. Similar decreases of N2A expression were observed with **2** by $33.08 \pm 15.5\%$ ($p = 0.09$) and with **3** by $43.1 \pm 7.6\%$ ($p < 0.05$). Moreover, no significant differences in the expression of the NMDA receptor subunit N2B were found between control and 3xTg-AD neurons and none of the compounds affected the N2B subunit expression as shown in Figure 7B. Also, the compounds did not induce any changes in the mGlu5 receptor expression as shown in Figure 7C, where the upper band corresponds to the receptor dimers.⁴⁷ The decrease in the expression of the NMDA 2A subunit induced by **1–3** suggest the involvement of this receptor in the gambierol effects. Moreover, our previous work had shown a relationship between NMDA receptors and the effects of **1** over intracellular calcium concentration.¹³ In fact, we have previously shown that the calcium oscillations induced by **1** and 4-AP in cerebellar neurons occurred mainly through NMDA receptor activation. Although we cannot rule out the possibility of direct interaction of **1** with glutamate receptors, it is known that potassium channel blockers can stimulate NMDA receptors.^{14,48} Therefore, we investigated if the co-treatment with the well-known NMDA receptor antagonist APV could block the observed effects. For this purpose, 3xTg-AD primary neurons were pretreated with APV at $100 \mu\text{M}$ either alone or in combination with **1**, and also with $20 \mu\text{M}$ of 6-cyano-7-nitroquinoxaline-2,3-dione (CNQX), an AMPA/kainate receptor antagonist, to evaluate the

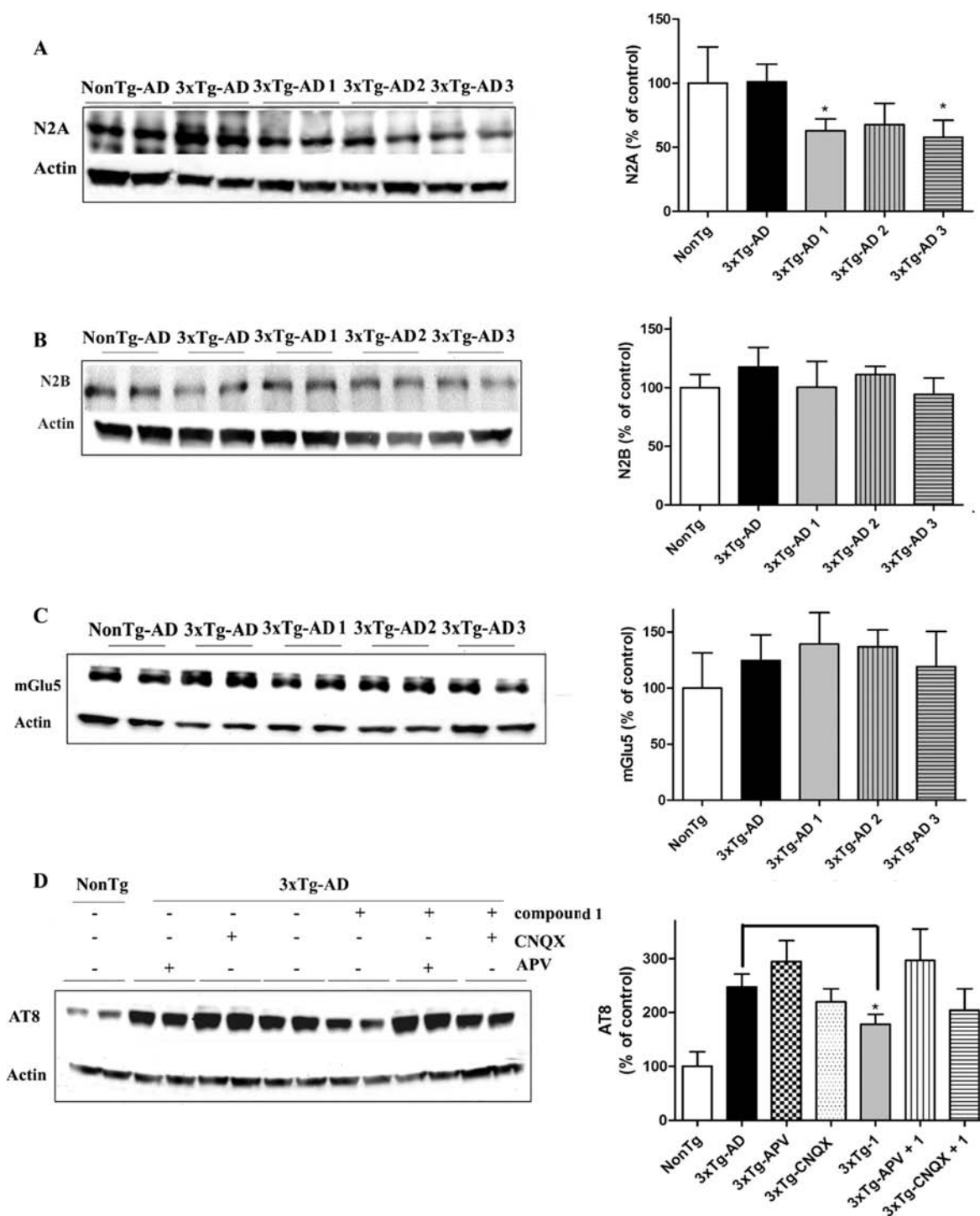


Figure 7. Chronic treatment with **1** induced changes in glutamate receptors expression. (A) Representative experiment showing Western blot bands for NMDA 2A subunit levels in control, 3xTg-AD, and treated 3xTg-AD neurons. Quantitative analysis of the effect on NMDA subunit 2A levels as obtained from 3 independent experiments. (B) Representative Western blot bands showing the effect of **1**, **2**, and **3** in the steady-state level of NMDA 2B subunit. Quantification of the data as obtained from five independent experiments indicating no effect of chronic pretreatment on N2B expression. (C) Representative experiment showing Western blot bands for mGlu5 levels in control, 3xTg-AD, and treated 3xTg-AD neurons. Quantitative analysis showing no effect of the pretreatments in mGlu5 levels expression as obtained from 3 independent experiments each performed in duplicate. (D) Representative Western blot bands for AT8 immunoreactivity (tau phosphorylated at Ser 199 and Ser 202) showing that pretreatment with APV but not with CNQX blocked the effect of **1** over AT8 levels expression as obtained from 3 independent experiments.

possible interaction of these glutamate receptors. In fact, the extracellular presence of APV fully blocked the effect of **1** over AT8 expression, while CNQX failed to block the action of **1** (Figure 7D), pointing to NMDA receptor implications in the effects of **1**.

DISCUSSION

The past decade has seen significant advances in total synthesis of marine polycyclic ether toxins.⁴⁹ However, skeletal SARs of marine polycyclic ether natural products have been underexplored because chemoselective modification/alteration of their

Table 1. List of Antibodies and Dilutions Used

antibody	immunogen	host	dilution	source
6E10	Aa 1–16 of A β	mouse	1:1000	Signet
AT8	Peptide with phospho-S199/S202/T205	mouse	1:1000	Pierce
AT100	Peptide with phospho-S212/T214	mouse	1:1000	Pierce
NMDA 2A	C-terminal fusion protein rat NMDAR2A aa.1253–1391	rabbit	1:1000	Millipore
NMDA 2B	NMDAR2B aa. 892–1051	mouse	1:500	BD Bioscience
mGluR5	Shyntenic peptide from rat mGluR5	rabbit	1:1000	Millipore
Actin	C-terminal actin fragment, clone C4	mouse	1:20000	Millipore

highly complicated skeletal structure is assumed to be virtually impossible. In this context, “diverted total synthesis”⁵⁰ is believed to be the only way to access designed skeletal analogues. Unfortunately, drastic simplification of the skeletal structure of marine polycyclic ether natural products without affecting their biological function has been a significant challenge at the interface of chemistry and biology. In fact, previous studies have not been successful in yielding truncated analogues with cellular activity.^{51–56}

Kopljar et al. showed that 1 μ M of gambierol (**1**, Figure 1) had no effect on K_{v2} or K_{v4} channels but it fully suppressed K_{v3.1} currents, showing a nanomolar affinity to K_{v3.1} and K_{v3.3} channels in transfected mouse fibroblasts.²¹ Furthermore, they also profoundly studied the binding of **1** to the chimeric K_{v2.1}/K_{v3.1} channels and found that **1** stabilized the closed state of potassium channels without acting as an external pore blocker or as an internal cavity blocker. It seems that **1** links to its binding site through the plasma membrane on the lipid-exposed face of the channel pore, stabilizing the closed state of the channel. Our previous SAR study has elucidated that the H-ring functionalities, including the partially skipped triene side chain, were found to be important for the potent acute toxicity against mice, while the A-ring functionalities had little influence on the activity. Taken together with the recent studies on the effects of gambierol on K_v channels,^{10–13,21} we hypothesized that the minimal skeletal structure required for potent K_v channel binding ability would reside in the right-half of the molecule. Accordingly, in the present study, we designed the heptacyclic and tetracyclic analogues (**2** and **3**, respectively, Figure 1), both of which contain all of the H-ring functionalities required for the potent toxicity, while their chemical synthesis is significantly easier than that of the natural product. Although it has long been believed that the full molecular length of the polycyclic ethers that reaches several nanometers in general may be critically important for their potent biological activity,^{51–56} the present study clearly demonstrates that only the right-half domain of **1** is necessary for the inhibition of K⁺ current and its beneficial effects in the 3xTg-AD cortical model.

In this work, we showed that the upregulation of K_{v3.1} subunit expression found in 3xTg-AD neurons is inhibited by long-term pretreatment with **1**, **2**, or **3**. Moreover, this decrease in K_{v3.1} expression in neurons cultured in the presence of the compounds was linked to a reduction in the peak amplitude of K_v currents in this cellular model. However, this effect was not observed in the corresponding wild-type nontransgenic cortical culture, where only long-term exposure of the neurons to **1** showed an inhibition of the I_{DR} component of the potassium current. In addition, acute administration of these compounds decreased the outward I_K current and also the delayed I_{DR} current by 35–50% at compound concentrations in the nanomolar range.

It is important to remark that we show for the first time that cortical 3xTg-AD neurons endogenously overexpress K_{v3.1} channels, which may be a consequence of the intra- and extracellular A β overexpression in these cultures. In this sense, it has been shown that extracellular administration of A β _{1–42} in human microglia and hippocampal primary neurons produces and upregulates K_{v3.1} and K_{v3.4} channels.^{57,58} Yu and colleagues showed that treatment of mouse cortical neurons with A β _{25–35} or A β _{1–42} fragments caused an enhancement of the outward K⁺ current, with a special upregulation of the delayed current and that the specific I_{DR} blocker tetraethylammonium (TEA) was able to protect these cells from A β induced cell death.⁵⁹

We have previously linked the gambierol-induced neuronal effects to functional modulation of NMDA receptors in primary cultures of cerebellar neurons.¹³ Although in this study **1** did not modify the glutamate-induced calcium increase, the compound causes a sustained increase in the intracellular calcium concentration in cortical neurons (Alonso et al., unpublished observations) which could be probably attributed to the interaction of the toxin with glutamate receptors. Overactivation of NMDA receptors can lead to neuronal damage through calcium overload,⁶⁰ but a high blockage also provokes neuronal dysfunction.⁶¹ Memantine is a low affinity NMDA antagonist widely used for the treatment of moderate to severe AD,⁶² which showed NMDA antagonism in micromolar concentrations⁶³ with beneficial effects in 3xTg-AD mice,⁶⁴ resulting in a decrease in the levels of A β and hyperphosphorylated tau. Furthermore, recent studies have indicated the involvement of NMDA receptors in APP expression and A β production.¹⁴ As shown in this work, **1–3** were also able to reduce these two cellular pathologies, decreasing both intra- and extracellular A β levels together with the amount of hyperphosphorylated tau recognized by AT8 and AT100 antibodies. As occurred with the intracellular calcium oscillations induced by **1** in cerebellar granule cells,¹³ the effects of **1** over AT8 expression were blocked by the preincubation of the cells with APV and also diminished in the presence of CNQX, pointing again to NMDA and AMPA/kainate receptors as mediators of the beneficial effect of these compounds on the AD pathology. Both A β peptides and even phosphorylated tau proteins are supposed to interact with NMDA receptors and to be implicated in the glutamate enhancement of AD pathology.⁶⁵ Although coincubation with NMDA and AMPA receptor modulators blocked the effects of **1** in this cellular system, further detailed investigation into the molecular mechanism of NMDA receptor modulation by **1** remains as a future challenge. Even though bioavailability studies to evaluate the ability of these compounds to cross the blood brain barrier are not available yet, a previous report with modified analogues of gambierol showed that these analogues produced neurological symptoms resembling those of **1**.^{9b}

Moreover, the results described here showing that two different analogues with different lengths showed the same effects as **1** and even with lower doses are important for the development of further studies to investigate the capacity of these compounds to cross the blood brain barrier.

CONCLUSIONS

In the present study, we designed and synthesized truncated skeletal analogues of gambierol (**1**) and showed that the inhibitory activity of **1** against K_v channels resides in the right-wing domain of the polycyclic ether skeleton. Our successful elaboration of structurally simplified skeletal analogues, that is, **2** and **3**, with potency comparable to that of **1** demonstrates the power of the concept of diverted total synthesis.⁶⁶ Furthermore, we have shown that compounds **1–3** lowered both intra- and extracellular $A\beta$ levels and tau hyperphosphorylation via modulation of NMDA receptors that is possibly secondary to K_v channel inhibition in an in vitro mouse model of AD. Thus, **1** and its skeletal analogues should serve as useful chemical probes for understanding the function of K_v channels and for elucidating the molecular mechanism of $A\beta$ metabolism modulated by NMDA receptors.

EXPERIMENTAL SECTION

Synthetic Chemistry. For details, see the Supporting Information.

Primary Cortical Neurons. Two colonies of homozygous 3xTg-AD mice and wild nontransgenic (NonTg) were established at the animal facilities of the University of Santiago de Compostela, Spain, where animals were used to obtain primary cultures of cortical neurons from 3xTg-AD and Nontransgenic mice. All protocols described in this work were revised and authorized by the University of Santiago de Compostela Institutional animal care and use committee.

Primary cortical neurons were obtained from embryonic day 15–17 NonTg and homozygous 3xTg-AD mice fetuses as recently described elsewhere.^{22,45,46} Briefly, cerebral cortex was removed and neuronal cells were dissociated by trypsinization followed by mechanical titration in DNase-containing solution (0.005% w/v) with a soybean trypsin inhibitor (0.05% w/v) at 37 °C. After dissociation, the cells were suspended in Dulbecco's Modified Eagle's medium (DMEM) supplemented with *p*-amino benzoic acid, insulin, penicillin, and 10% fetal calf serum. The cell suspension was seeded in 12 or 96 multiwell plates precoated with poly-D-lysine and incubated for 7–10 days in vitro (div) in a humidified 5% CO₂/95% air atmosphere at 37 °C. Cytosine arabinoside, 20 μM, was added before 48 h of culture to prevent growing of non-neuronal cells. In all the experiments, cortical neurons from NonTg and 3xTg-AD mice were prepared and processed simultaneously.

Chemicals and Solutions. Plastic tissue-culture dishes were obtained from Falcon (Madrid, Spain). Fetal calf serum was purchased from Gibco (Glasgow, U.K.) and DMEM was from Biochrom (Berlin, Germany). Fura-2 acetoxymethyl ester (Fura 2-AM) was from Molecular Probes (Leiden, The Netherlands). All other chemicals were reagent grade and purchased from Sigma-Aldrich (Madrid, Spain).

Synthetic gambierol and analogues were purified by HPLC prior to biological experiments. Copies of HPLC traces are included in the Supporting Information. Dimethylsulfoxide (DMSO) was used for the preparation of gambierol and analogue stock solutions. The final DMSO concentration in the extracellular culture medium was always lower than 0.05%.

Western Blotting. Cultured neurons pretreated with the compounds from the third to the seventh div were lysed in 50 mM Tris-HCl buffer (pH 7.4) containing a phosphatase/protease cocktail inhibitor (Roche). The protein concentration in the lysates was determined by the Bradford assay. Samples of cell lysates containing 20 μg of total protein were resolved in gel loading buffer (50 mM Tris-HCl, 100 mM dithiothreitol, 2% SDS, 20% glycerol, 0.05%

bromophenol blue, pH 6.8) by SDS-PAGE and transferred onto PVDF membranes (Millipore). The Snap i.d. protein detection system was used for blocking and antibody incubation as previously described.²² The concentrations of primary antibodies employed in this work are shown in Table 1.

The immunoreactive bands were detected using the Supersignal West Pico chemiluminescent substrate (Pierce) and the Diversity 4 gel documentation and analysis system (Syngene, Cambridge, U.K.). Chemiluminescence was measured with the Diversity GeneSnap software (Syngene). β -Actin was used as control for lane loading and to normalize chemiluminescence values.

ELISA. The amount of amyloid β in the culture medium was measured with the Colorimetric BetaMark x-42 ELISA kit (SIGNET) following the protocol indicated by the manufacturer. The human $A\beta$ 1–42 peptide used in this kit shows an estimated 21% cross-reactivity with rodent $A\beta$ 1–42 peptide. In all the experiments, culture medium samples were obtained at the same days in vitro from NonTg and 3xTg-AD cultures after the treatment with the compounds from third to seventh div. The optical density was measured at 620 nm in a Syngene multiwell plate reader.

Determination of the Cytosolic Calcium Concentration [Ca^{2+}]_c. Cultured cortical neurons from NonTg and 3xTg-AD mice treated with the compounds from third to seventh div were loaded with the Ca^{2+} sensitive fluorescent dye Fura-2 AM at 2.5 μM for 10 min at 37 °C. Then, cells were washed 3 times with cold buffer. The coverslips were inserted into a thermostatted chamber at 37 °C (Life Science Resources, Royston, Herts, U.K.) and viewed with a Nikon Diaphot 200 microscope equipped with epifluorescence optics (Nikon 40×-immersion UV-Fluor objective). The [Ca^{2+}]_c images were collected by doubled excitation fluorescence with a Life Science Resources equipment. The light source was a 175 W xenon lamp. The calibration of the fluorescence was made by the Grynkiewicz method. For the calcium experiments, the extracellular medium contained (in mM): 154 NaCl, 5.6 KCl, 1.3 CaCl₂, 1 MgCl₂, 5.6 glucose, and 10 HEPES, pH 7.4 adjusted with Tris. All experiments were carried out in duplicate.

Electrophysiology. Potassium currents were recorded from primary cortical neurons at room temperature (22–25 °C), using a computer-controlled amplifier (Multiclamp 700B, Molecular Devices; Sunnyvale, CA). Signals were recorded and analyzed using a Pentium computer equipped with the Digidata 1440 data acquisition system and pClamp10 software (Molecular Devices). Signals were prefiltered at 5 kHz and digitized using a Digidata 1200 interface (Axon Instruments).

In most experiments, the patch-clamp technique in whole-cell configuration was performed using borosilicate glass micropipets of 5–10 MΩ resistance. The internal pipet solution contained (in mM): 132.5 KCl, 0.6 EGTA, 10 HEPES, 2 MgCl₂, 2 ATP, and 0.3 GTP, pH 7.2 adjusted with KOH. The extracellular solution contained (in mM): 154 NaCl, 5.6 KCl, 3.6 NaHCO₃, 1.3 CaCl₂, 1 MgCl₂, 5 glucose, and 10 HEPES, pH 7.2. To eliminate sodium currents, saxitoxin at 1 μM was added to the extracellular solution in all the experiments testing potassium currents.

To isolate the inactivating component I_A and the delayed-rectifier noninactivating component I_{DR} of K^+ currents, previously described electrophysiological protocols were used.⁵⁸ Total outward current ($I_K = I_A + I_{DR}$) was measured by applying a depolarizing voltage step from –100 to +40 mV of 250 ms duration, preceded by a preconditioning pulse at –100 mV of 1.5 s from a holding potential of –80 mV. Then, after a conditioning pulse at –40 mV during 100 ms, for full inactivation of the I_A component, the I_{DR} current was isolated by applying a depolarizing step from –40 to +40 mV.

Determination of Cell Viability. Cell viability was assessed by the MTT (3-[4,5-dimethylthiazol-2-yl]-2,5-diphenyltetrazolium bromide) test, as previously described.^{45,46} This test, which measures mitochondrial function, was used to assess cell viability as it has been shown that in neuronal cells there is a good correlation between a drug-induced decrease in mitochondrial activity and its cytotoxicity. The assay was performed in cultures grown in 96 well plates and exposed to different concentrations of **1**, **2**, or **3** added to the culture

medium. Cultures were maintained in the presence of the compounds at 37 °C in humidified 5% CO₂/95% air atmosphere for 120 h. Sodium azide was used as cellular death control and its fluorescence was subtracted to the other data. After the exposure time, cells were rinsed and incubated for 60 min with a solution of MTT (500 μg/mL) dissolved in Locke's buffer containing (in mM): 154 NaCl, 5.6 KCl, 1.3 CaCl₂, 1 MgCl₂, 5.6 glucose, and 10 HEPES, pH 7.4 adjusted with Tris. After washing off excess MTT, the cells were disaggregated with 5% sodium dodecyl sulfate and the colored formazan salt was measured at 590 nM in a spectrophotometer plate reader.

Statistical Analysis. All data are expressed as means ± SEM of three or more experiments (each performed in duplicate). Statistical comparison was by nonpaired Student's *t* test or ANOVA with Dunnett's multiple comparison test. *P*-values <0.05 were considered statistically significant.

Abbreviations. 3xTg, Triple transgenic; 4-AP, 4-aminopyridine; Aβ, amyloid β peptide; Ac, acetyl; AD, Alzheimer's Disease; AIBN, α,α'-azobisisobutyronitrile; APP, amyloid-β precursor protein; APV, D-(-)-2-amino-5-phosphonopentanoate; BACE, β-secretase; CNQ X, 6-cyano-7-nitro-quinoxaline-2,3-dione; COD, 1,5-cyclooctadiene; CSA, (±)-10-camphorsulfonic acid; div, days in vitro; DIBALH, diisobutylaluminum hydride; DMEM, Dulbecco's modified Eagle's medium; DMAP, 4-dimethylaminopyridine; DMF, *N,N*-dimethylformamide; DMSO, dimethylsulfoxide; Kv, voltage-gated potassium channel; LHMDs, lithium bis(trimethylsilyl)amide; mGluR, metabotropic glutamate receptor; MPM, *p*-methoxyphenylmethyl; MS, molecular sieves; MTT, 3-[4,5-dimethylthiazol-2-yl]-2,5-diphenyltetrazolium bromide; Nav, voltage-gated sodium channel; NaHMDS, sodium bis(trimethylsilyl)amide; NIS, *N*-iodosuccinimide; NMDA, *N*-methyl-D-aspartate; NMO, *N*-methylmorpholine *N*-oxide; nonTg, non Triple transgenic; OTf, trifluoromethanesulfonate; PbTxs, brevetoxins; PPTS, pyridinium *p*-toluenesulfonate; Py, pyridine; SAR, structure-activity relationship; TBAF, tetra-*n*-butylammonium fluoride; TBS, tert-butyltrimethylsilyl; TEA, tetraethylammonium; THF, tetrahydrofuran; TMS, trimethylsilyl; TPAP, tetra-*n*-propylammonium perruthenate.

■ ASSOCIATED CONTENT

● Supporting Information

Synthetic procedure, compound characterization data, and copies of ¹H and ¹³C NMR spectra for all new compounds. This material is available free of charge via the Internet at <http://pubs.acs.org>.

■ AUTHOR INFORMATION

Corresponding Author

*Luis.Botana@usc.es

Notes

The authors declare no competing financial interest.

■ ACKNOWLEDGMENTS

This work was funded with the following grants. From Ministerio de Ciencia y Tecnología, Spain: AGL2007-60946/ALI, SAF2009-12581 (subprograma NEF), AGL2009-13581-CO2-01, TRA2009-0189, AGL2010-17875. From Xunta de Galicia, Spain: GRC 2010/10, PGDIT 07MMA006261PR, PGDIT (INCITE) 09MMA003261PR, PGDIT (INCITE) 09261080PR, 2009/XA044, 2009/053 (Consell. Educación), 2008/CP389 (EPITOX, Consell. Innovación e Industria, programa IN.CI.TE.), 10PXIB261254 PR. From EU VIIth Frame Program: 211326 - CP (CONFIDENCE), 265896 BAMMBO, 265409 μAQUA, and 262649 BEADS. From the Atlantic Area Programme (Interreg IVB Trans-national): 2008-1/003 (Atlantox) and 2009-1/117 Pharamatlantic. From the Ministry of Education, Culture, Sports, Science and Technology (MEXT), Japan: Grants-in-Aid for Young Scientists (B) and for Scientific Research on Innovative Areas "Chemical Biology of

Natural Products". From Japan Society for the Promotion of Science (JSPS), Japan: Grants-in-Aid for Young Scientists (A) and for Scientific Research (A). Eva Alonso is recipient of a predoctoral fellowship from Fondo de Investigaciones Sanitarias (pFIS), Ministerio de Sanidad y Consumo, Spain.

■ REFERENCES

- (1) Lin, Y.-Y.; Risk, M.; Ray, S. M.; Van Engen, D.; Clardy, J.; Golik, J.; James, J. C.; Nakanishi, K. *J. Am. Chem. Soc.* **1981**, *103*, 6773.
- (2) For review see: (a) Yasumoto, T.; Murata, M. *Chem. Rev.* **1993**, *93*, 1897. (b) Murata, M.; Yasumoto, T. *Nat. Prod. Rep.* **2000**, *17*, 293.
- (3) Ito, E.; Suzuki-Toyota, F.; Toshimori, K.; Fuwa, H.; Tachibana, K.; Satake, M.; Sasaki, M. *Toxicol.* **2003**, *42*, 733.
- (4) Satake, M.; Murata, M.; Yasumoto, T. *J. Am. Chem. Soc.* **1993**, *115*, 361.
- (5) (a) Fuwa, H.; Sasaki, M.; Satake, M.; Tachibana, K. *Org. Lett.* **2002**, *4*, 2981. (b) Fuwa, H.; Kainuma, N.; Tachibana, K.; Sasaki, M. *J. Am. Chem. Soc.* **2002**, *124*, 14983.
- (6) (a) Kadota, I.; Takamura, H.; Sato, K.; Ohno, A.; Matsuda, K.; Yamamoto, Y. *J. Am. Chem. Soc.* **2003**, *125*, 46. (b) Kadota, I.; Takamura, H.; Sato, K.; Ohno, A.; Matsuda, K.; Satake, M.; Yamamoto, Y. *J. Am. Chem. Soc.* **2003**, *125*, 11893.
- (7) (a) Johnson, H. W.; Majumder, U.; Rainier, J. D. *J. Am. Chem. Soc.* **2005**, *127*, 848. (b) Majumder, U.; Cox, J. M.; Johnson, H. W.; Rainier, J. D. *Chem.—Eur. J.* **2006**, *12*, 1736. (c) Johnson, H. W.; Majumder, U.; Rainier, J. D. *Chem.—Eur. J.* **2006**, *12*, 1747.
- (8) Furuta, H.; Hasegawa, Y.; Mori, Y. *Org. Lett.* **2009**, *11*, 4382.
- (9) (a) Furuta, H.; Hasegawa, Y.; Hase, M.; Mori, Y. *Chem.—Eur. J.* **2010**, *16*, 7586. (b) Fuwa, H.; Kainuma, N.; Satake, M.; Sasaki, M. *Bioorg. Med. Chem. Lett.* **2003**, *13*, 2519. (c) Fuwa, H.; Kainuma, N.; Tachibana, K.; Tsukano, C.; Satake, M.; Sasaki, M. *Chem.—Eur. J.* **2004**, *10*, 4894.
- (10) Ghiaroni, V.; Sasaki, M.; Fuwa, H.; Rossini, G. P.; Scalera, G.; Yasumoto, T.; Pietra, P.; Bigiani, A. *Toxicol. Sci.* **2005**, *85*, 657.
- (11) Cuyppers, E.; Yanagihara, A.; Rainier, J. D.; Tytgat, J. *Biochem. Biophys. Res. Commun.* **2007**, *361*, 214–17.
- (12) Cuyppers, E.; Abdel-Mottaleb, Y.; Kopljar, I.; Rainier, J. D.; Raes, A. L.; Snyders, D. J.; Tytgat, J. *J. Toxicol.* **2008**, *51* (6), 974–83.
- (13) Louzao, M. C.; Cagide, E.; Vieytes, M. R.; Sasaki, M.; Fuwa, H.; Yasumoto, T.; Botana, L. M. *Cell. Physiol. Biochem.* **2006**, *17*, 257.
- (14) LePage, K. T.; Rainier, J. D.; Johnson, H. W.; Baden, D. G.; Murray, T. F. *J. Pharmacol. Exp. Ther.* **2007**, *323*, 174.
- (15) Alonso, E.; Vale, C.; Sasaki, M.; Fuwa, H.; Konno, Y.; Perez, S.; Vieytes, M. R.; Botana, L. M. *J. Cell. Biochem.* **2010**, *110*, 497.
- (16) (a) Verges, D. K.; Restivo, J. L.; Goebel, W. D.; Holtzman, D. M.; Cirrito, J. R. *J. Neurosci.* **2011**, *31*, 11328. (b) Bordji, K.; Becerril-Ortega, J.; Nicole, O.; Buisson, A. *J. Neurosci.* **2010**, *30*, 15927. (c) Hoey, S. E.; Williams, R. J.; Perkinson, M. S. *J. Neurosci.* **2009**, *29*, 4442.
- (17) Ballatore, C.; Lee, V. M.; Trojanowski, J. Q. *Nat. Rev. Neurosci.* **2007**, *8*, 663.
- (18) Hardy, J. A.; Higgins, G. A. *Science* **1992**, *256*, 184.
- (19) Selkoe, D. J. *Science* **1997**, *275*, 630.
- (20) Goedert, M.; Wischik, C. M.; Crowther, R. A.; Walker, J. E.; Klug, A. *Proc. Natl. Acad. Sci. U.S.A.* **1988**, *85*, 4051.
- (21) Pendlebury, W. W.; Solomon, P. R. *Clin. Symp.* **1996**, *48*, 2.
- (22) Spillantini, M. G.; Goedert, M. *Trends Neurosci.* **1998**, *21*, 428.
- (23) Kopljar, I.; Labro, A. J.; Cuyppers, E.; Johnson, H. W.; Rainier, J. D.; Tytgat, J.; Snyders, D. J. *Proc. Natl. Acad. Sci. U.S.A.* **2009**, *106*, 9896.
- (24) Vale, C.; Alonso, E.; Rubiolo, J. A.; Vieytes, M. R.; LaFerla, F. M.; Gimenez-Llort, L.; Botana, L. M. *Cell. Mol. Neurobiol.* **2010**, *30*, 577.
- (25) Fuwa, H.; Noji, S.; Sasaki, M. *J. Org. Chem.* **2010**, *75*, 5072.
- (26) For reviews see: (a) Hoveyda, A. H.; Zhugralin, A. R. *Nature* **2007**, *450*, 243. (b) Gradillas, A.; Perez-Castells, J. *Angew. Chem., Int. Ed.* **2006**, *45*, 6086. (c) Nicolaou, K. C.; Bulger, P. G.; Sarlah, D.

- Angew. Chem., Int. Ed.* **2005**, *44*, 4490. (d) Deiters, A.; Martin, S. F. *Chem. Rev.* **2004**, *104*, 2199.
- (25) Watanabe, W. H.; Conlon, L. E. *J. Am. Chem. Soc.* **1957**, *79*, 2828.
- (26) Bosch, M.; Schlaf, M. *J. Org. Chem.* **2003**, *68*, 5225.
- (27) Okimoto, Y.; Sakaguchi, S.; Ishii, Y. *J. Am. Chem. Soc.* **2002**, *124*, 1590.
- (28) Scholl, M.; Ding, S.; Lee, C. W.; Grubbs, R. H. *Org. Lett.* **1999**, *1*, 953.
- (29) (a) Sasaki, M.; Fuwa, H.; Inoue, M.; Tachibana, K. *Tetrahedron Lett.* **1998**, *39*, 9027. (b) Sasaki, M.; Fuwa, H.; Ishikawa, M.; Tachibana, K. *Org. Lett.* **1999**, *1*, 1075. (c) Sasaki, M.; Ishikawa, M.; Fuwa, H.; Tachibana, K. *Tetrahedron* **2002**, *58*, 1889.
- (30) For reviews see: (a) Fuwa, H. *Synlett* **2011**, *6*. (b) Fuwa, H. *Bull. Chem. Soc. Jpn.* **2010**, *83*, 1401. (c) Sasaki, M.; Fuwa, H. *Nat. Prod. Rep.* **2008**, *25*, 401. (d) Sasaki, M. *Bull. Chem. Soc. Jpn.* **2007**, *80*, 856.
- (31) Ley, S. V.; Norman, J.; Griffith, W. P.; Marsden, S. P. *Synthesis* **1994**, *1994*, 639.
- (32) Fuwa, H.; Sasaki, M.; Tachibana, K. *Org. Lett.* **2001**, *3*, 3549.
- (33) Nicolaou, K. C.; Prasad, C. V. C.; Hwang, C. K.; Duggan, M. E.; Veale, C. A. *J. Am. Chem. Soc.* **1989**, *111*, 5321.
- (34) Kobayashi, S.; Hori, M.; Hirama, M. *Carbohydr. Res.* **2008**, *343*, 443.
- (35) Ito, Y.; Hirao, T.; Saegusa, T. *J. Org. Chem.* **1978**, *43*, 1011.
- (36) Feng, F.; Murai, A. *Chem. Lett.* **1992**, 1587.
- (37) Uenishi, J. i.; Kawahama, R.; Yonemitsu, O.; Tsuji, J. *J. Org. Chem.* **1998**, *63*, 8965.
- (38) Stille, J. K. *Angew. Chem., Int. Ed. Engl.* **1986**, *25*, 508.
- (39) Han, X.; Stoltz, B. M.; Corey, E. J. *J. Am. Chem. Soc.* **1999**, *121*, 7600.
- (40) Schwab, P.; Grubbs, R. H.; Ziller, J. W. *J. Am. Chem. Soc.* **1996**, *118*, 100.
- (41) Lau, A.; Tymianski, M. *Pflugers Arch.* **2010**, *460*, 525.
- (42) Oddo, S.; Caccamo, A.; Tseng, B.; Cheng, D.; Vasilevko, V.; Cribbs, D. H.; LaFerla, F. M. *J. Neurosci.* **2008**, *28*, 12163.
- (43) De Felice, F. G.; Wu, D.; Lambert, M. P.; Fernandez, S. J.; Velasco, P. T.; Lacor, P. N.; Bigio, E. H.; Jerecic, J.; Acton, P. J.; Shughrue, P. J.; Chen-Dodson, E.; Kinney, G. G.; Klein, W. L. *Neurobiol. Aging* **2008**, *29*, 1334.
- (44) Guo, J. P.; Arai, T.; Miklossy, J.; McGeer, P. L. *Proc. Natl. Acad. Sci. U.S.A.* **2006**, *103*, 1953.
- (45) Alonso, E.; Vale, C.; Vieytes, M. R.; Laferla, F. M.; Gimenez-Llort, L.; Botana, L. M. *Neurochem. Int.* **2011**, *59*, 1056.
- (46) Alonso, E.; Vale, C.; Vieytes, M. R.; Laferla, F. M.; Gimenez-Llort, L.; Botana, L. M. *Cell. Physiol. Biochem.* **2011**, *27*, 783.
- (47) Romano, C.; Yang, W. L.; O'Malley, K. L. *J. Biol. Chem.* **1996**, *271*, 28612.
- (48) Hardingham, G. E.; Fukunaga, Y.; Bading, H. *Nat. Neurosci.* **2002**, *5*, 405.
- (49) For reviews see: (a) Nicolaou, K. C.; Aversa, R. J. *Isr. J. Chem.* **2011**, *51*, 359. (b) Nicolaou, K. C.; Frederick, M. O.; Aversa, R. J. *Angew. Chem., Int. Ed.* **2008**, *47*, 7182. (c) Inoue, M. *Chem. Rev.* **2005**, *105*, 4379. (d) Nakata, T. *Chem. Rev.* **2005**, *105*, 4314.
- (50) For review see: Szpilman, A. M.; Carreira, E. M. *Angew. Chem., Int. Ed.* **2010**, *49*, 9592.
- (51) (a) Rein, K. S.; Baden, D. G.; Gawley, R. E. *J. Org. Chem.* **1994**, *59*, 2101. (b) Gawley, R. E.; Rein, K. S.; Jeglitsch, G.; Adams, D. J.; Theodorakis, E. A.; Tiebjes, J.; Nicolaou, K. C.; Baden, D. G. *Chem. Biol.* **1995**, *2*, 533.
- (52) (a) Inoue, M.; Hirama, M.; Satake, M.; Sugiyama, K.; Yasumoto, T. *Toxicon* **2003**, *41*, 469. (b) Inoue, M.; Lee, N.; Miyazaki, K.; Usuki, T.; Matsuoka, S.; Hirama, M. *Angew. Chem., Int. Ed.* **2008**, *47*, 8611.
- (53) (a) Torikai, K.; Oishi, T.; Ujihara, S.; Matsumori, N.; Konoki, K.; Murata, M.; Aimoto, S. *J. Am. Chem. Soc.* **2008**, *130*, 10217. (b) Torikai, K.; Yari, H.; Mori, M.; Ujihara, S.; Matsumori, N.; Murata, M.; Oishi, T. *Bioorg. Med. Chem. Lett.* **2006**, *16*, 6355. (c) Ujihara, S.; Oishi, T.; Torikai, K.; Konoki, K.; Matsumori, N.; Murata, M.; Oshima, Y.; Aimoto, S. *Bioorg. Med. Chem. Lett.* **2008**, *18*, 6115.
- (54) Sasaki, M.; Tachibana, K. *Tetrahedron Lett.* **2007**, *48*, 3181.
- (55) Oguri, H.; Tanabe, S.; Oomura, A.; Umetsu, M.; Hirama, M. *Tetrahedron Lett.* **2006**, *47*, 5801. (b) Oguri, H.; Oomura, A.; Tanabe, S.; Hirama, M. *Tetrahedron Lett.* **2005**, *46*, 2179.
- (56) Candenias, M. L.; Pinto, F. M.; Cintado, C. G.; Morales, E. Q.; Brouard, I.; Díaz, M. T.; Rico, M.; Rodríguez, E.; Rodríguez, R. M.; Pérez, R.; Pérez, R. L.; Martín, J. D. *Tetrahedron* **2002**, *58*, 1921.
- (57) Franciosi, S.; Ryu, J. K.; Choi, H. B.; Radov, L.; Kim, S. U.; McLarnon, J. G. *J. Neurosci.* **2006**, *26*, 11652.
- (58) Pannaccione, A.; Boscia, F.; Scorziello, A.; Adornetto, A.; Castaldo, P.; Sirabella, R.; Tagliatalata, M.; Di Renzo, G. F.; Annunziato, L. *Mol. Pharmacol.* **2007**, *72*, 665.
- (59) Yu, S. P.; Farhangrazi, Z. S.; Ying, H. S.; Yeh, C. H.; Choi, D. W. *Neurobiol. Dis.* **1998**, *5*, 81.
- (60) Albers, G. W.; Goldberg, M. P.; Choi, D. W. *Arch. Neurol.* **1992**, *49*, 418.
- (61) Collingridge, G. L.; Bliss, T. V. *Trends Neurosci.* **1995**, *18*, 54.
- (62) Reisberg, B.; Doody, R.; Stoffler, A.; Schmitt, F.; Ferris, S.; Mobius, H. J. *N. Engl. J. Med.* **2003**, *348*, 1333.
- (63) Parsons, C. G.; Stoffler, A.; Danysz, W. *Neuropharmacology* **2007**, *53*, 699.
- (64) Martinez-Coria, H.; Green, K. N.; Billings, L. M.; Kitazawa, M.; Albrecht, M.; Rammes, G.; Parsons, C. G.; Gupta, S.; Banerjee, P.; LaFerla, F. M. *Am. J. Pathol.* **2010**, *176*, 870.
- (65) Hu, N. W.; Ondrejcek, T.; Rowan, M. J. *Pharmacol., Biochem. Behav.* **2012**, *100*, 855.
- (66) For successful examples of skeletal truncation of structurally complex natural products, see: (a) Wender, P. A.; Baryza, J. L.; Brenner, S. E.; DeChristopher, B. A.; Loy, B. A.; Schrier, A. J.; Verma, V. A. *Proc. Natl. Acad. Sci. U.S.A.* **2011**, *108*, 6721. (b) Schnermann, M. J.; Beaudry, C. M.; Egorova, A. V.; Polishchuk, R. S.; Sutterlin, C.; Overman, L. E. *Proc. Natl. Acad. Sci. U.S.A.* **2010**, *107*, 6158. (c) Bonazzi, S.; Eidam, O.; Guttinger, S.; Wach, J. Y.; Zemp, I.; Kutay, U.; Gademann, K. *J. Am. Chem. Soc.* **2010**, *132*, 1432. (d) Shan, D.; Chen, L.; Njardarson, J. T.; Gaul, C.; Ma, X.; Danishefsky, S. J.; Huang, X. Y. *Proc. Natl. Acad. Sci. U.S.A.* **2005**, *102*, 3772. (e) Kishi, Y.; Fang, F.; Forsyth, C.; Scola, P.; Yoon, S. Patent, U., Ed. 1995; Vol. 5436238.